

## Investigating extracellular polymeric substances from microbial mat upon exposure to sunlight



Mashura Shammi<sup>a,b,f</sup>, Xiangliang Pan<sup>a,e,\*</sup>, Khan M.G. Mostofa<sup>c,\*\*</sup>, Daoyong Zhang<sup>a</sup>, Cong-Qiang Liu<sup>d</sup>, Wenjuan Song<sup>a</sup>

<sup>a</sup> Laboratory of Bioremediation, Department of Environmental Pollution and Process Control, Xinjiang Institute of Ecology and Geography, Chinese Academy of Sciences, Urumqi 830011, Xinjiang, PR China

<sup>b</sup> Department of Environmental Sciences, Jahangirnagar University, Dhaka 1342, Bangladesh

<sup>c</sup> Institute of Surface-Earth System Science, Tianjin University, 92 Weijin Road, Nankai District, Tianjin 300072, PR China

<sup>d</sup> State Key Laboratory of Environmental Geochemistry, Institute of Geochemistry, Chinese Academy of Sciences, Guiyang 550002, Guizhou, PR China

<sup>e</sup> College of Environment, Zhejiang University of Technology, Hangzhou 310014, Zhejiang, PR China

<sup>f</sup> University of Chinese Academy of Sciences, Beijing 100049, PR China

### ARTICLE INFO

#### Keywords:

Microbial mat  
Extracellular polymeric substance (EPS)  
Photodegradation  
Dissolved organic carbon (DOC)  
Excitation-emission matrix (EEM) spectroscopy  
Parallel factor (PARAFAC) modelling

### ABSTRACT

Microbial mat extracellular polymeric substances (EPS) and their fate and transformation in natural waters are unidentified under diurnal condition. EPS from highly saline arid origins were characterised and exposed to natural sunlight conditions to identify its physico-chemical changes over 72 h. Fourier Transform Infrared Spectroscopy (FTIR) and potentiometric titration analyses confirmed the presence of –COOH and –OH functional groups in raw EPS. In addition, size exclusion chromatography (SEC) confirmed the presence of two proteins-sized molecules in the original EPS which were found to degrade upon sunlight exposure. The excitation-emission matrix (EEM) and parallel factor (EEM-PARAFAC) identified two fluorescent components: A combined humic-like and protein-like component, and an individual tyrosine-like component. FTIR in irradiated samples confirmed degradation of EPS by showing presence of the –CH<sub>3</sub> group at 1377 cm<sup>-1</sup>. Two proteins-sized molecules identified in SEC were degraded, thereby causing to significant changes in the pH and redox potential (Eh). Correspondingly, three fluorescent components were identified in irradiated samples using EEM-PARAFAC modelling and found to change in their fluorescence intensities upon sunlight exposure. It is therefore suggested that photochemical processes are important for sequential transformation of EPS into various organic substances in surface waters.

### 1. Introduction

Bacterial biofilms are formed by communities that are embedded in a self-produced matrix of extracellular polymeric substances (EPS). Importantly, bacteria in biofilms exhibit a set of prominent properties that differ substantially from free-living bacterial cells [1]. Biofilm microbial communities of microbial cells provide protective environments for the cells that inhabit the biofilm, enabling them to respond efficiently to the environmental challenges [2]. Microbial mats, on the other hand, are structured, small-scale microbial ecosystems, and similar as biofilms cover a substratum like a tissue [3]. Microbial mats, on the other hands, are vertically stratified communities that host a complex consortium of microorganisms, dominated by cyanobacteria

that compete for available nutrients and environmental niches, within these extreme habitats [4]. In addition a general characteristic of a microbial mat is the steep physicochemical gradients that are the result of the metabolic activities of the mat microorganisms. Virtually every microbial mat is formed through autotrophic metabolism and through the fixation of atmospheric dinitrogen. Chemoautotrophic organisms fuel these processes in the absence of light. In illuminated environments photoautotrophic organisms are the driving force [3].

EPS, a self-produced matrix of microorganisms, are composed of mainly polysaccharides (40–90%), proteins, nucleic acids, lipids, and humic-like component [5,6]. EPS are high molecular weight mixture of polymers, approximately molecular-weight MW of 410,000 Da [7,8] and other cellular components [7] secreted by bacteria and various

\* Corresponding author. Laboratory of Bioremediation, Department of Environmental Pollution and Process Control, Xinjiang Institute of Ecology and Geography, Chinese Academy of Sciences, Urumqi 830011, Xinjiang, PR China.

\*\* Corresponding author. Institute of Surface-Earth System Science, Tianjin University, 92 Weijin Road, Nankai District, Tianjin 300072, PR China.

E-mail addresses: [xiangliangpan@163.com](mailto:xiangliangpan@163.com) (X. Pan), [mostofa@tju.edu.cn](mailto:mostofa@tju.edu.cn) (K.M.G. Mostofa).

<http://dx.doi.org/10.1016/j.polydegstab.2017.10.011>

Received 25 May 2017; Received in revised form 14 October 2017; Accepted 17 October 2017

Available online 19 October 2017

0141-3910/ © 2017 Elsevier Ltd. All rights reserved.

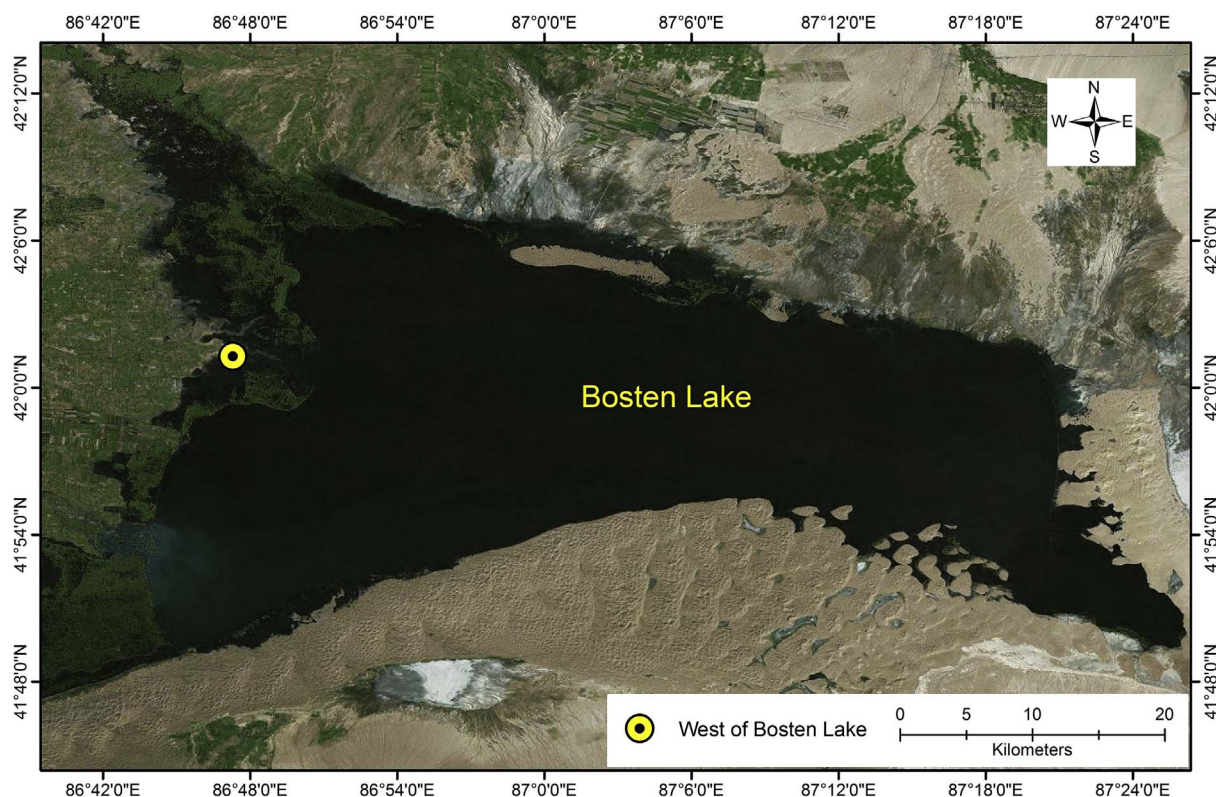


Fig. 1. Sampling site of saline pond near Bosten Lake. Sampling point shown in yellow mark. (For interpretation of the references to colour in this figure legend, the reader is referred to the web version of this article.)

heteropolymers [9]. EPS constitute a large and dynamic pool of dissolved organic carbon (DOC) in freshwater lake and oceanic environments [10,11]. DOC comprises the largest pool of actively cycling organic carbon (C) as dissolved organic matter (DOM) in aquatic ecosystems [12,13]. Previous studies have confirmed that simulated solar radiation at varying levels of dissolved oxygen and under different incident light wavelength regimes had destroyed high-molecular-weight (HMW) fractions of DOM and formed low-molecular-weight (LMW) constituents [14,15]. The protein-like fraction of EPS displayed a wide range of MW ( $> 600$  kDa –  $< 10$  kDa) whereas the humic-like fraction was composed of molecules of LMW (6.0 –  $< 1.2$  kDa) in earlier studies [16].

EPS of microbial origin are one of the major components of natural organic matter in natural waters [17]. It plays multiple functions, including aggregation of bacterial cells, cohesion of biofilms, retention of water, sorption of organic and inorganic components, nutrient source, exchange of genetic information, and so on [6]. They have chains that hydrate on contact with water, the feature that gives them their physical properties [18]. It is known that EPS are biodegradable by their own producers and by other microorganisms when they are starved, as a substrate for microorganisms, and that the EPS carbohydrate can be utilized faster than the EPS protein [19] as a source of energy and nutrition. Recently it has been reported that artificial UVB irradiation increased the fluorescence intensity of all the protein and tyrosine-like peaks of EPS from *Chroococcus minutus* while UVC irradiation had little effect [20]. Nevertheless, another study of the same research group further suggested that EPS protein was vulnerable to UVB radiation compared to the EPS polysaccharides [21], thereby contradicting their previous study. Beforehand, it was reported that bulk DOM was degraded by sunlight which subsequently formed into a variety of photoproducts [15]. Correspondingly, solar radiation has been reported to result in photomineralization of chromophoric dissolved organic matter (CDOM) or fluorescent DOM (FDOM), or in photo-humification, and photo-formation of reactive oxygen species in waters [22–25].

Fluorescence spectroscopy was used to characterize dissolved organic matter (DOM) in concentrated and unconcentrated water samples from a wide variety of freshwater, coastal and marine environments. Several types of fluorescent signals were observed, including humic-like, tyrosine-like and tryptophan-like [26]. Differences in humic peak A and C suggested that the humic material in marine surface waters was chemically different from humic material in the other environments sampled [26]. Moreover, development of parallel factor (PARAFAC) modelling on the excitation-emission matrix (EEM) spectra (EEM-PARAFAC) was applied to distinguish the new fluorescent components in DOM [11,27] and CDOM [11,29,30] in the freshwater and marine environments to isolate and quantify the individual fluorescence component signals in terms of fluorescence intensity. EEM-PARAFAC modelling is a three-way multivariate analysis, which has been applied extensively on an additive mixture of fluorescence signals obtained from EEM spectra [31–33]. Recently EEM-PARAFAC has been used to characterize EPS components [35] and flocculation of EPS components [57].

Until now the fate of microbial mat EPS and their fate and transformation into FDOM components are still not well defined under diurnal condition. In what way the presence of sunlight and night conditions affects the behavior of EPS in terms of chemical and spectroscopic studies is still unexplored. EEM-PARAFAC can be applied to distinguish the new fluorescent components formed in irradiated EPS. This study uses chemical analyses to examine photochemical changes in terms of physico-chemical properties like pH and redox potential Eh, contents of dissolved organic carbon (DOC), the functional groups and molecular weight of EPS. Furthermore, the changes in fluorescent components in EPS were identified using a combination of EEM spectra and PARAFAC modelling in order to examine their environmental fate.

## 2. Materials and methods

### 2.1. Collection of microbial mats

Microbial mat samples rich in EPS was collected from the “little lake” west of Bosten lake (N42°01.269' and E86°47.293'), which has higher salinity than that of Bosten Lake (Fig. 1) on May 28, 2014. The little lake is a complex channel network overgrown by thick reeds [34]. In addition, agriculture wastewater drainage is discharged into the lake at its northwest corner, and this leads to the highest salinity (about  $3.0 \text{ g L}^{-1}$ ) [36] as well as high DOC content in the water that varied from  $84.5 \pm 0.6 \text{ mg/L}$  to  $100.8 \pm 0.1 \text{ mg/L}$  in the summer [35]. A large steel mug of long stick was used to collect the floating biofilm mat from the lake water. The chunks of biofilm mats were put in a drum of 30 L with lake water. After transportation to laboratory they were stored in a plastic zip bag of 500 mL and preserved at  $-20 \text{ }^\circ\text{C}$  for further processing.

### 2.2. Extraction of EPS from microbial mats

Micorbial mats were washed at least 10 times with MQ water before EPS extraction. As from the previous study of Pan et al. [37], it was found that pretreatment with ultrasound at low intensity doubled the EPS yield without significant modification of the composition of EPS [37]. Therefore ultrasonication as a physical method was chosen for extraction of EPS from biofilm as described from previous methods [38]. The sonicated microbial mat suspension was then centrifuged at  $16,000 \text{ r/min}$ , at  $4 \text{ }^\circ\text{C}$  for 20 min [39]. The EPS extraction method would not cause any cell lysis [39]. The supernatants were filtered through a  $0.22 \text{ }\mu\text{m}$  polycarbonate filters. The filtrate was used as the EPS sample. This method of extraction increases total EPS yield without modifying EPS molecule and includes whole EPS without differentiating tightly-bound or loosely-bound EPS. Approximately 180 g wet weight biofilm of approximately 200 mL had obtained near about 150 mL EPS. The EPS solution was stored at  $-20 \text{ }^\circ\text{C}$  until further use. The 150 mL solution was diluted three times to 450 mL in total and used in subsequent photo experiment.

### 2.3. EPS characterization

The quantities of polysaccharides in EPS samples were determined by the phenol-sulfuric acid method where glucose was used as a standard substance [40]. Absorbance was measured at 488 nm against blank to determine the polysaccharide in this study. Protein content of the EPS was determined using modified Lowry procedure for room temperature with bovine serum albumin (BSA) as a standard (Sengon Biotech, Shanghai) [41]. In protein analysis, absorbance of the samples was measured at 750 nm against blank. A calibration curve was prepared before each analysis. A UV spectrophotometer (UV – 2550, SHIMADZU) was used in both measurements. DOC was measured by Analyticjena multi N/C 2100 (Germany). No filtration was conducted before DOC as EPS was extracted by centrifugation followed by filtration with  $0.22 \text{ }\mu\text{m}$  filter paper. pH and redox potential Eh ( $-\text{mV}$ ) were measured by pH meter (MetroOhm).

### 2.4. Potentiometric titration

Acid–base titrations were performed using an automatic potentiometric titrator (Metrohm Titrino 702SM). Potentiometric titrations of concentrated  $440 \text{ mg/L}$  EPS of 40 mL suspensions were carried out under a  $\text{N}_2$  atmosphere at  $25 \text{ }^\circ\text{C}$ . The suspension was titrated using  $0.1 \text{ M NaOH}$  solutions. A known amount of  $0.1 \text{ M HCl}$  was further added at the beginning of the experiment to lower the pH to approximately 1.6 and equilibrated in room temperature overnight and then titrated to pH 12 with NaOH [42]. Therefore, the total adsorption sites ( $1.5 \leq \text{pKa} \leq 12.0$ ) concentration on the adsorbents surface was

calculated according to the changes in the pH values of the suspension and the amount of added OH. At each titration step a stability of  $0.1 \text{ mVS}^{-1}$  was attained before the addition of the next dripping of titrant. Blank titrations were performed using  $0.1 \text{ M KNO}_3$ .

### 2.5. Photo-experiment set up for light incubation

Dissolved organic carbons (DOC) of EPS were diluted with MilliQ water to adjust DOC of lake water which varied from  $80 \text{ mgL}^{-1}$  to  $120 \text{ mgL}^{-1}$ . To examine the effects of solar radiation on EPS, three Erlenmeyer glass flasks were filled with the EPS samples (150 mL), sealed with glass caps and Teflon tapes. The flasks were kept in a water bath, in which tap water was continuously supplied to control the temperature. The samples were exposed to natural sunlight from a period of 0 h–72 h. Every 15 min all flasks were shaken and their positions randomised. The photo-experiment was started at 10:15 a.m., 8th July and ended at 10:15 a.m. of 11th July 2014. The experiment was set on the roof of the Xinjiang Institute of Ecology and Geography, Urumqi, China. Day length was approximately 15.17 h. Sample exposure to sunlight was approximately 6 h each day (10:15 a.m. to 4:00 p.m.). UV intensity of the experimental day varied from 10 to  $15 \text{ Wm}^{-2}$  on the first day of exposure followed by  $7\text{--}9 \text{ Wm}^{-2}$  on the 2nd and 3rd day. Air temperature varied from  $20 \text{ }^\circ\text{C}$  to  $31 \text{ }^\circ\text{C}$ . Data were taken from Urumqi Ambiente Previsión índice (website: <http://www.qx121.cn/qxfw/ASP/wlmqzwx.asp>). The photo active radiation (PAR) value was measured with a quantam meter (Model ESM-Q1, Ecotron Scientific Inc.) in  $\mu\text{mol m}^{-2}\text{s}^{-1}$ . PAR varied from  $1041 \mu\text{mol m}^{-2}\text{s}^{-1}$  at 10:15 a.m. to approximately  $1985 \mu\text{mol m}^{-2}\text{s}^{-1}$  at 2:00 p.m. At 4:00 p.m. PAR was approximately  $1500 \mu\text{mol m}^{-2}\text{s}^{-1}$ . Water bath temperature was measured with a thermometer. Incubated samples were withdrawn in triplicate from flasks in 20 ml at 0.5 h, 1 h, 2 h, 6 h, 24 h, 48 h and 72 h for further analysis.

### 2.6. Fourier Transform Infrared Spectroscopy (FTIR) analysis

EPS samples were freeze-dried at  $-70 \text{ }^\circ\text{C}$  and the dried samples were mixed with solid KBr in the ratio of 1:100. From the mixture, KBr–EPS pellets 13 mm in diameter were prepared at  $8.103 \text{ kg cm}^{-2}$  pressure. The FTIR spectra of the EPS samples were recorded with Bruker Tensor 27 and analysed with OPUS software 5.5. For each interferogram 256 scans were taken in the  $400\text{--}4000 \text{ cm}^{-1}$  range with a resolution of  $2 \text{ cm}^{-1}$ . The processed spectra were exported to Origin 8.0 software (OriginLab, USA) for graph preparation.

### 2.7. Size exclusion chromatography (SEC)

Protein molecular weight of EPS was qualitatively determined. A Merck Hitachi LA Chrom Chromatograph equipped with a L2200 auto sampler, a L2130 quaternary pump, a L2300 column oven interface and a L2455 diode array UV detector (200–600 nm), with software version LaChrom 890–8800–12 was used. An Amersham Biosciences column, Superdex 200 10/300 GL, was used (resolving range from 10 to 600 kDa). Data processing was done with EZchrom Elite. The mobile phase recommended elsewhere [16,43]. Injection volume was  $80 \mu\text{L}$  EPS. Molecular weight  $14.4 \text{ kDa}\text{--}94.7 \text{ kDa}$  was used for qualitative protein analysis which contained protein markers of 94 kDa, 66.2 kDa, 45 kDa, 33 kDa, 26 kDa, 20 kDa and 14.4 kDa (TIANGEN MP102, Sengong Biotech). The entire 3 injections obtained 5 peak positions in the chromatogram according to the standard markers in retention time 18.27–22.08 min, 29.42–32.38 min, 40.42–41.83 min, 50.58–52.41 min and 58.20–62.01 min, respectively. After obtaining the standard peak the sample injections were run as without exposure to sunlight (original EPS) and after exposure to sunlight.

## 2.8. EEM-PARAFAC modelling

The fluorescence (excitation – emission matrix, EEM) spectra of the EPS solution were recorded with a fluorescence spectrophotometer (F-4500, HITACHI, Japan) in scan mode with a 700-voltage xenon lamp at room temperature. The EEM spectra were collected at 5 nm increments over an excitation range of 200–400 nm, with an emission range of 250–500 nm by every 1 nm. The excitation and emission slits were set to 5 nm of band-pass, respectively. The scan speed was  $1200 \text{ nm min}^{-1}$ . All the cuvettes before analysis were rinsed and ultra-sonicated using 5% (w/w) nitric acid solution. The Milli-Q water blank was subtracted from the sample's EEM spectra. To clarify the changes in the chemical and spectroscopic analyses of photochemical and microbial degradation of EPS, we conducted PARAFAC modelling on the EEM spectra of EPS samples.

## 2.9. Anion and cation analysis

Ion chromatograph (US Dionex ICS-5000), and inductively coupled plasma emission spectroscopy (Agilent 735 ICP-OES) for major anions ( $\text{Cl}^-$ ,  $\text{SO}_4^{2-}$  and  $\text{HCO}_3^-$ ) and cations ( $\text{Ca}^{2+}$ ,  $\text{Mg}^{2+}$ ,  $\text{K}^+$  and  $\text{Na}^+$ ) analysis. Samples were filtered with  $0.45 \mu\text{m}$  syringe filter prior to sample analysis. EPS sample was filtered with  $0.45 \mu\text{m}$  polycarbonate filter and was not acidified. Standard curves were obtained containing known concentrations of each heavy metal that were diluted with Milli-Q pure water. All reagents were of analytical grade. The standard error was determined to be less than 5%. All glassware used for trace element analysis were soaked in 25%  $\text{HNO}_3$  for 24 h, rinsed, and then dried.

## 2.10. Dark control experiment

A control experiment on EPS degradation was performed in a dark room temperature, wherein flasks were wrapped with aluminium foils. EPS samples were collected at 0 h, 6 h, 48 h and 72 h. There were no significant changes observed for DOC, FTIR and EEM-PARAFAC modelling.

## 2.11. Statistical analysis

All incubation of EPS sample in the sunlight was triplicated. EPS characterizations were performed thrice and standard errors on measured values were calculated. The data were processed in Origin 8.0 software (OriginLab, USA) for graph preparation.

## 3. Results and discussions

### 3.1. Changes in EPS proteins and associated physico-chemical characteristics

Total protein content, total polysaccharide content and DOC content in EPS solution were  $60.6 \pm 3 \text{ mgL}^{-1}$  and  $23.2 \pm 0.5 \text{ mgL}^{-1}$  and  $392.7 \pm 3 \text{ mgL}^{-1}$ , respectively. Potentiometric titration of original EPS revealed two apparent dissociation constants (pKa values) in EPS (Fig. 2). The first equivalence point  $\text{EP}_1$  obtained at pH 4.99 was attributed to protein content of carboxylic groups [42,44]. The second equivalence point,  $\text{EP}_2$  obtained at pH 7.83, can be assigned to phenolic hydroxyl in protein substances [45,46]. Previous report from Sonicated EPS had shown phenolic hydroxyl pKa value at around 8.7 [45,46].  $\text{EP}_2$  may also belong to the phenolic hydroxyl groups of humic substances which was mentioned as 8.29 [47] and 8.8 [48].

Protein molecular weight (MW) study using size exclusion chromatography (SEC) also revealed presence of two protein sizes in the original EPS (Fig. 3). The chromatogram of untreated EPS exhibited two peaks—a large major peaks followed by a minor peaks. A small sub-peak was also observed before the major peak in untreated EPS. The peaks may be attributed to MW of 94.7–66.2 kDa of 82.58% and

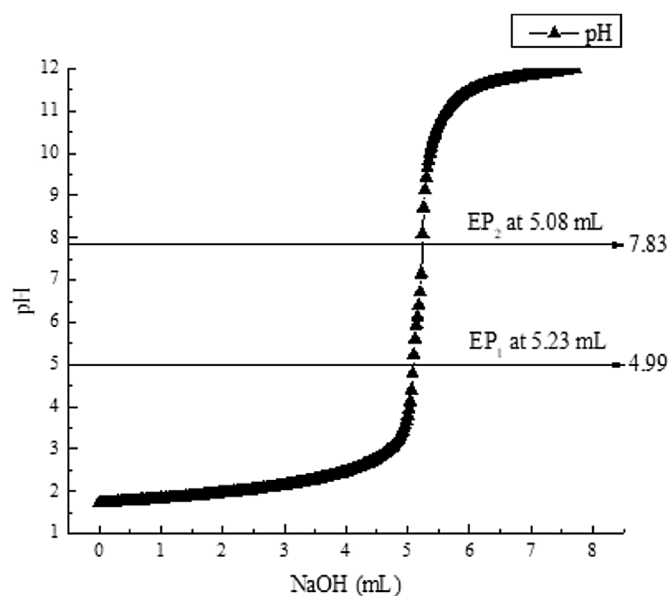


Fig. 2. Potentiometric titration curves for EPS collected from hypersaline biofilm mat. EP indicates the equivalence points on the titration curve. Potentiometric titrator (Metrohm Titrino 702SM) automatically generated two EP points as EP1 and EP2 (with two pH points) which are expressed in the Figure. No colour indicators were used during titration.

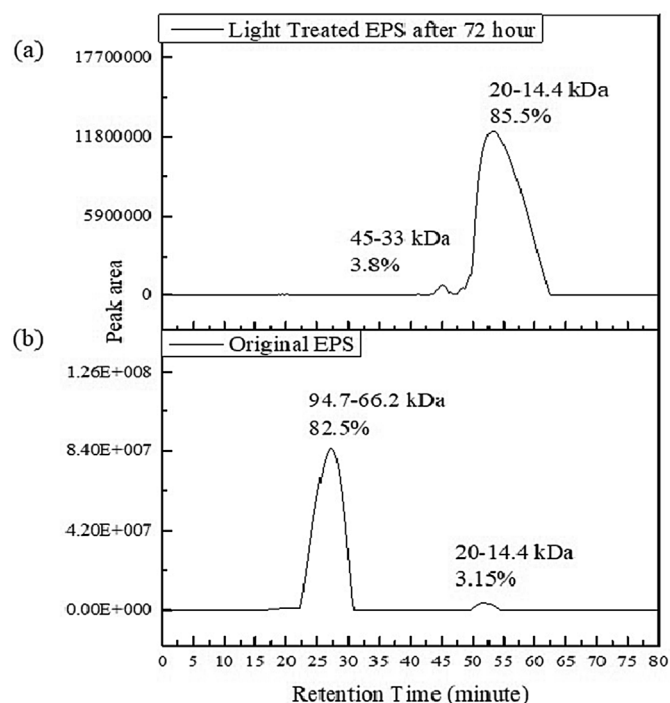


Fig. 3. Fingerprints of EPS before and after sunlight exposure of after 72 hours. EPS without exposure obtained three peaks with different retention times, including 15.2–20.8, 21.0–21.8 and 48–52 min, respectively. After three days of light exposure obtained three peaks and their retention times were 21.0–21.8, 42.5–43.0 and 47.6–62.3 min, respectively.

20.0–14.4 kDa, approximately 3.15%, respectively. After 72 h of sunlight exposure, treated EPS also showed two peak positions but reverse in order compared to the original EPS. A minor peak followed by a major peak was observed in the chromatogram. In both cases a small sub-peak was observed similar to that of original EPS. The two peaks, which may be assigned to 45–33 kDa protein with a peak area percentage of 3.76% and 20.0–14.4 kDa protein molecules with a peak area percentage of 85.56%, respectively. This is suggestive of the

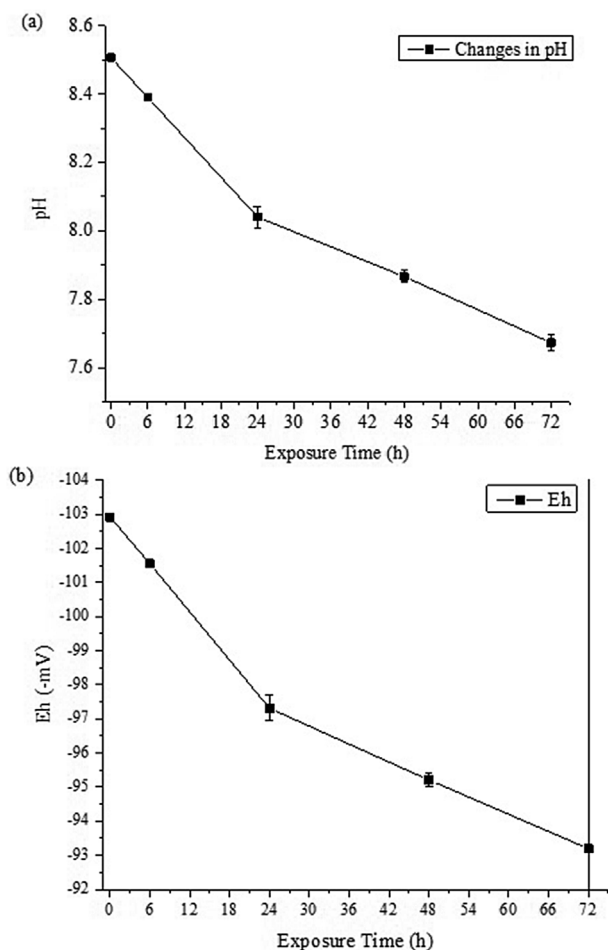


Fig. 4. Changes in pH (a) and Eh (b) in light treated sample during the exposure time.

maximal photo-induced alterations of HMW protein components of EPS into LMW components (Fig. 3). It is a key indicator of photochemical EPS alterations. The shoulders and sub-peaks representative of the low MW fractions in the original samples either increased in intensity or were replaced by new shoulders and sub-peaks, implying a net formation of LMW fractions, among which an important component could be organic acids [14,15]. Similar results were also found upon sunlight exposure on DOM in surface waters [27]. Previously microbial changes in the HMW components of EPS were also reported, whereas carbohydrates and proteins in EPS had entirely decomposed microbially during the experiment [19].

The pH of the EPS was alkaline ( $8.51 \pm 0.03$ ), possibly due to its origin from highly alkaline lake water which varied from pH 8.53–8.75. During the irradiation time pH and Eh of the sample EPS shifted over the course of 72 h and approximately 10.9% decrease in pH and Eh was observed in light-treated samples compared to the original untreated EPS (Fig. 4a). Redox potential Eh also decreased correspondingly (Fig. 4b). The decrease in pH and correspondingly redox potential Eh was presumably due to the formation of acidic photoproducts from EPS. Previously it was reported that due to the formation of acidic photoproducts with pKa values lower than the DOM's initial pH values caused lowering of pH [14]. Reduction of pH and decrease in protein molecular size was also reported in previous studies [36]. Similar phenomena might have affected EPS samples during irradiation.

### 3.2. Chemical and molecular changes in EPS during photolysis

Constituent of EPS protein content and its changes were further revealed from FTIR spectrum. FTIR spectra (Fig. 5) of the extracted EPS

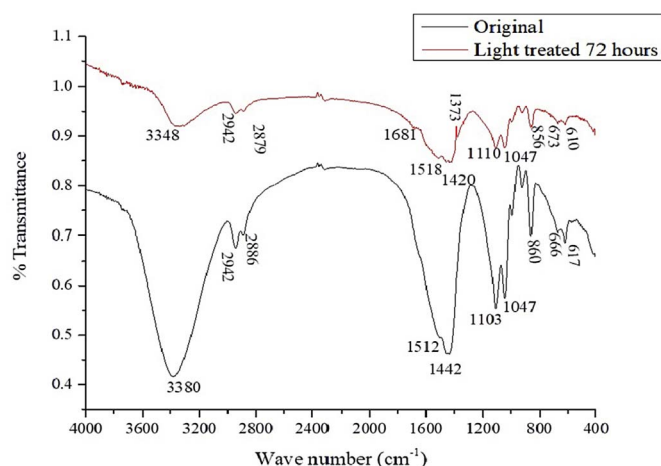


Fig. 5. FTIR spectra of the untreated EPS and light treated EPS after 72 hours.

and photo-treated EPS showed several major infrared absorption bands, which are the characteristics of the major functional groups bound in various molecules composing EPS. The broad and strong band around  $3700 \text{ cm}^{-1}$  to  $3000 \text{ cm}^{-1}$  indicates the stretching of O–H similar to all polymers. The bands at 2943 and  $2888 \text{ cm}^{-1}$  in EPS corresponded to the C–H stretching vibration of methyl and methylene groups [49]. Proteins are shown by the two bands at  $1440 \text{ cm}^{-1}$  in original EPS, and  $1403 \text{ cm}^{-1}$  in irradiated EPS after 72 h. This may be assigned to the –NH (bending vibration), –CN (stretching vibration) of Amide I band. Another weak peak positioned at around  $1510\text{--}1518 \text{ cm}^{-1}$  in original EPS and treated EPS may belong to C–O stretching vibration of carboxylic acid derivatives [50]. Two strong peaks around  $1048 \text{ cm}^{-1}$  and  $1112 \text{ cm}^{-1}$  can be signals for all esters and may belong to carbohydrates. Other major peak regions include  $600\text{--}921 \text{ cm}^{-1}$  similar to the carbohydrates and polysaccharides belonging to the glycosidic linkage of sugar monomers [50].

After 72 h of sunlight exposure, most of the absorption bands in IR spectra were substantially band-shifted and reduced in terms of peak heights, particularly over the fingerprint regions at  $1300\text{--}1600 \text{ cm}^{-1}$ , along with slight changes in peak positions (Fig. 5). This suggests an obvious change in the functional groups bound in carbohydrates and proteins. A new medium-strong peak appeared at  $\sim 1377 \text{ cm}^{-1}$  can be assigned to the signal of –CH<sub>3</sub> groups [50]. However, this position may also correspond to vibration of C=N. Similar peaks were observed in EPS (at  $1350 \text{ nm}^{-1}$ ) when Ethylenediaminetetraacetic acid (EDTA) as extractant and in the Suwannee River DOM at  $\sim 1370 \text{ cm}^{-1}$  [51,52]. Previously it was reported that proteins and carbohydrates are generally labile to microbial degradation either in EPS or DOM in water [19,51]. The changes in FTIR spectrum indicate that a significant change in the molecular structure of EPS molecules occurred upon sunlight exposure. This is further confirmed by subsequent changes in DOC.

A decrease of 6.9% DOC was observed within first 6 h in treated EPS samples (Fig. 6). However, after 48 h and 72 h of EPS diurnal exposure, no significant changes in DOC was observed. It might be correspond to the origin of the EPS from microbial mats of arid saline lakes that have significant ability to resist UVB radiation. Previously the higher tolerance to UVB radiation of the desert cyanobacterium was reported before which was attributed to the higher resistance of its EPS to photo-degradation compared to the other aquatic species [21]. Moreover, the dilution effect of DOC and shorter exposure hours, in contrast to the previous study of longer exposure hours of EPS [55] might be also responsible for lower degradation of DOC. Original EPS DOC  $392.7 \pm 3 \text{ mg/L}$  was diluted to  $103.5 \pm 1 \text{ mg/L}$  by adding MQW to adjust with the lake water DOC concentration. This dilution of DOC might further lead to the formation of recalcitrant DOC after 6 h of

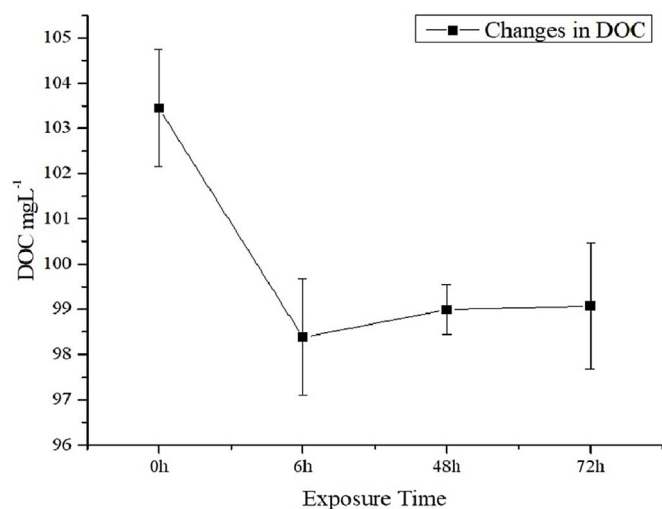


Fig. 6. Changes in the dissolved organic carbon (DOC) concentrations in irradiated samples at different time intervals.

exposure that resisted further degradation over the next days of exposures. It is therefore, obvious that arid saline lake microbial mats resist photodegradation significantly.

### 3.3. Genesis of new FDOM components and their changes during EPS photo-assimilation

The EEM-PARAFAC results confirmed that raw EPS composed of two fluorescent components (Fig. 7a–b; Table 1). The first fluorescent component represented a combined humic-like and protein-like component with four fluorescent peaks. Humic-like peaks were represented by two peaks: Peak M at Ex/Em = 275/410 nm and Peak A at Ex/

Em = 230/410 nm, respectively, and protein-like peaks were represented by: Peak T at Ex/Em = 270/335 nm and Peak Tuv at Ex/Em = 225/335 nm, respectively. The second fluorescent component was identified as individual tyrosine-like substances that consisted of two peaks represented by, Peak T at Ex/Em = 260/310 nm and Peak Tuv at Ex/Em = 220/310 nm, respectively. These results suggest that proteins and humic-like substances along with tyrosine-like components are the two major fluorescent components in raw EPS from microbial mats. Previous report also confirms that early summer development of microbial mats contained more protein-like and tyrosine- or tryptophan-like components along with humic-like substances [35]. It is therefore, evident that protein-like, humic-like [11,23,35,53] and tyrosine-like components are the important fluorescent molecular constituents of EPS molecular structure from microbial mats along with polysaccharides and other non-fluorescent components. Previously combined humic-like and protein like fluorescent component along with individual humic-like and unknown components were reported from aged microbial mats collected in winter [35]. It is apparent that protein-like substances of the microbial mat EPS and humic-like substances from the lake sediments [5], two major backbone of EPS fluorescent component, could have similar functional groups (–COOH and –NH<sub>2</sub>) [11], which might be responsible to interact with each other and produced combined fluorescent peaks [55].

On the other hand, the EEM-PARAFAC modelling in irradiated samples identified three fluorescent components, namely humic-like (Fig. 7c), tyrosine-like (Fig. 7d) and protein-like (Fig. 7e), during short-term irradiation (1–12 h). During long-term irradiation (24 h–72 h) EEM-PARAFAC modelling identified two components, namely tyrosine like (Fig. 7f) and protein-like (Fig. 7g; Table 1). After 72 h of sunlight exposure, humic-like components entirely decomposed as identified in the EEM-PARAFAC; meanwhile, the fluorescence intensity of the tyrosine-like component decreased by 5% but protein-like fluorescence increased by 27%. Decomposition of humic-like components is generally observed in surface waters [22,28], but the increase in the

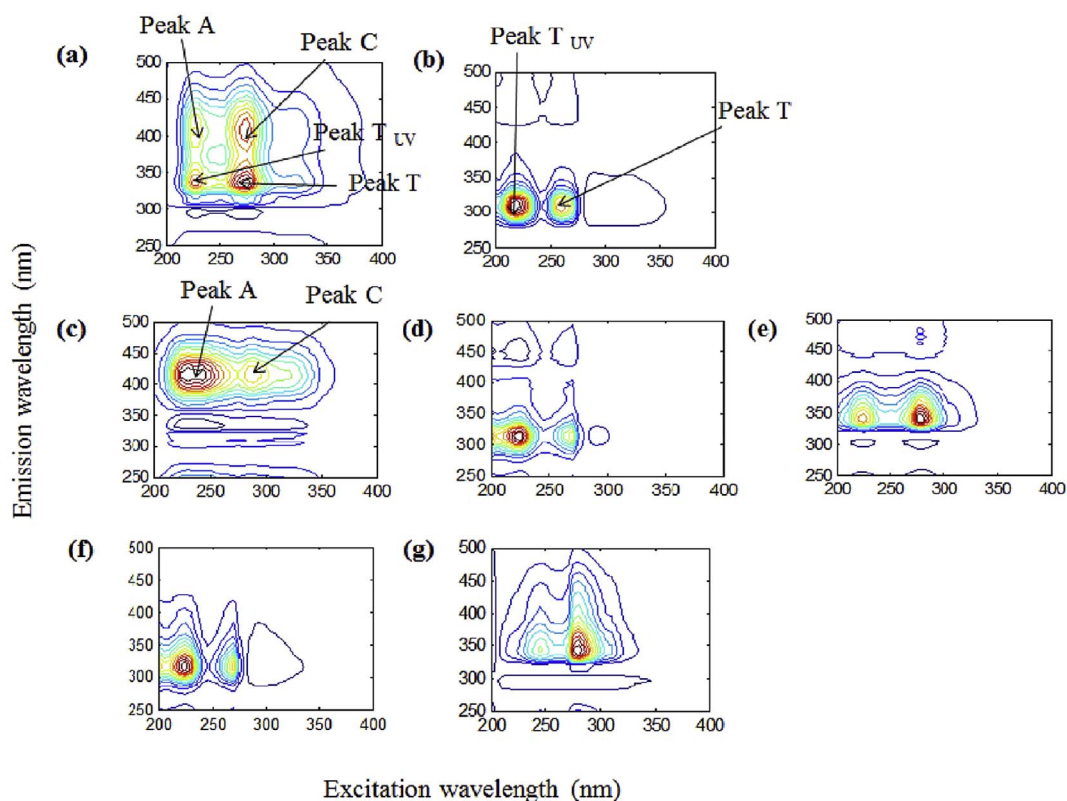


Fig. 7. Fluorescent components identified by PARAFAC modelling; (a-b) two fluorescent components for raw EPS solutions; (c-e) three fluorescent components for short term irradiation 0.5 hours to 12 hours; and (f-g) for relatively long-term irradiation for 24 hours to 72 hours.

**Table 1**

Fluorescence excitation/emission (Ex/Em) wavelengths of various components identified from EEM-PARAFAC modelling of raw EPS samples and irradiated EPS samples using EEM-PARAFAC modelling. The percentage changes in the fluorescence intensities of various components are estimated by comparing the treated samples with raw EPS samples.

Components	Excitation and emission maxima (% decrease in fluorescence intensity)	Description	Peak region	Corresponding description in the earlier studies
<b>Raw EPS sample fluorescence properties</b>				
Component 1 [35,54]	270/335 and 225/335	Protein-like	Peak T Peak T <sub>UV</sub>	280-300/328–356 nm [24] 235-250/338-356- nm [24]
	275/410 and 230/410	Humic-like	Peak M	310/423–428 [22]; 322/407 [26]; 290–330/358-416 nm [24]
Component 2	260/310 and 220/310	Tyrosine-like	Peak A Peak T Peak T <sub>UV</sub>	250-260/380–480 [22]; 225–260/358-416 nm [24] 275/310 [22]; 275/306 [29] In this study
	<b>Sunlight irradiated EPS (1 h to 12 h) in this study</b>			
Component 1	270/340 (–29%) 220/340 (–29%)	Protein-like	Peak T	270-280/320–350 [22]; 280/368 [27]
			Peak T <sub>UV</sub>	240/368 [27]
Component 2	285/415 (–78%) 225/415 (–78%)	Humic-like	Peak M	310/423–428 [22]; 322/407 [26]; 290-330/358–416 nm [24]
			Peak A	250-260/380–480 [22]; 225-260/358–416 nm [24]
Component 3	265/315 (–6%) 225/315 (–6%)	Tyrosine-like	Peak T	275/310 [22]; 275/306 [29]
			Peak T <sub>UV</sub>	In this study
<b>Sunlight irradiated EPS (24 h to 72 h) in this study</b>				
Component 1	280/340 (+27%) 245/340 (+27%)	Protein-like	Peak T	280-300/328–356 nm [24]
			Peak T <sub>UV</sub>	235-250/338-356- nm [24]
Component 2	270/315 (–5%) 225/315 (–5%)	Tyrosine-like	Peak T	275/310 [22]; 275/306 [29]
			Peak T <sub>UV</sub>	In this study

(+) and (–): an increase and a decrease in fluorescence intensities (%) of various peaks.

protein-like component may presumably result from the decomposition of humic-like components that are associated with protein-like components in raw EPS (Fig. 7a–b; Table 1). FDOM components typically undergo photochemical transformation but they are recalcitrant to microbial degradation, except for the aromatic amino acids that are microbiologically degraded under dark conditions [22,23,53]. The peak positions of the humic-like component were obviously red-shifted from the shorter to the longer wavelength regions from the raw EPS to the irradiated samples (Table 1; Fig. 7). Red-shift of the humic-like component could be linked with two possible phenomena: First, the humic-like component is released from EPS where it is typically bound with other molecules that could have less influence on photon absorption upon light exposure. Second, the humic-like component of photo-induced and/or microbial origin may compose of diverse functional groups, which may be produced during the respiration or assimilation processes of EPS.

Therefore, changes in FTIR spectrum, DOC, EEM-PARAFAC modelling, decrease in EPS MW during the irradiation period is related to the formation of low MW organic acids that correspondingly decreased solution pH and Eh in the EPS sample. These results indicate that photo-induced alterations of EPS caused structural changes of EPS proteins, carbohydrates and also a decrease in the molecular size of EPS. Production of LMW components could be the key signature of EPS alterations under photo-induced and its sequential release of new DOM in waters. However, no significant changes in DOC, FTIR and EEM-PARAFAC modelling were observed in the dark room control treatment during the experimental time period.

### 3.4. Environmental significance

The photodegradation of EPS may vary based on the origin of the microorganisms that produced it. In this regard saline water microbial

mat from arid origin showed lower degradation rate of DOC and protein fluorescence components within the exposure period. Previously it was reported that the desert cyanobacterium species *C. minutus* EPS protein showed higher tolerance to UVB degradation compared to the other aquatic species [19]. During photodegradation EPS-bound anions and cations may release and make complex again. From the concentration of some ion analysis in EPS (Table 2), it was observed that the content of  $\text{SO}_4^{2-}$  and  $\text{HCO}_3^-$  was higher EPS samples. Irradiated EPS showed decreased concentration of  $\text{HCO}_3^-$  indicating some mineralization of DOC. Significant changes in  $\text{SO}_4^{2-}$  concentration was also observed compared to the original EPS.  $\text{Cl}^-$  content in original and treated samples remained unchanged. Slight increase of  $\text{Ca}^{2+}$  and  $\text{K}^+$  ions in irradiated EPS was observed. In the natural microbial mat EPS may chelate with  $\text{Ca}^{2+}$  ions perhaps preventing the precipitation of  $\text{CaCO}_3$  [54]. Similarly, the degradation of EPS by heterotrophic bacteria may release  $\text{Ca}^{2+}$  and influence  $\text{CaCO}_3$  precipitation [55] as well as the other metals in the solution. In this case photo irradiation of EPS released  $\text{Ca}^{2+}$  and  $\text{K}^+$  ions from EPS-metal chelates. It was evident from

**Table 2**  
Changes in important ion concentration in EPS after 72 h of irradiation.

Concentration (mg/L)	0 h untreated EPS	72 h Irradiated EPS
$\text{Ca}^{2+}$	8.8 ± 0.1	10.4 ± 0.1
$\text{Mg}^{2+}$	31.2 ± 0.3	26.4 ± 0.02
$\text{K}^+$	9.6 ± 0.2	12.8 ± 0.7
$\text{Na}^+$	22.0 ± 0.9	19.6 ± 0.1
$\text{HCO}_3^-$	222.0 ± 0.4	198.5 ± 0.1
$\text{Cl}^-$	42.0 ± 0.2	42.0 ± 0.6
$\text{SO}_4^{2-}$	35.2 ± 1	30.4 ± 0.6

EEM-PARAFAC modelling that degradation of humic substances from raw EPS might have increased the  $\text{Ca}^{2+}$  and  $\text{K}^+$  ions in the solution. On the other hand decreased concentration of  $\text{Mg}^{2+}$  and  $\text{Na}^+$  ions may indicate their chelation by the remaining EPS proteins or the FDOM that remained in the solution. EPS may also serve to bind different heavy metal from the surrounding lake water. In the raw EPS sample significant concentration of several metals were found Fe (452.9 ppb), Zn (10.07 ppb), Al (2.78 ppb), Cr (3.5 ppb), Ni (12.6 ppb), As (35.05 ppb), Cd (0.01 ppb), Ba (15.22 ppb), Pb (0.4 ppb). The high abundance of EPS containing microbial mat may be effectively chelate large amounts of dissolved heavy metals. EPS proteins may serve as binding sites for many trace metals such as Cd, Cu and Pb [45–48], Hg (II) [56], Sb(v) [56,57]. Upon changes in temperature, pH [57], diurnal effect of sunlight exposure might degrade EPS into LMW organic acids and release the anions and cations back into the environment. The importance of this study is therefore linked to the photochemistry and biogeochemistry of microbial mat EPS and their fate in natural waters in inland saline lake environments.

It is evident that the anthropogenic modifications of aquatic environments, including nutrient over-enrichment (eutrophication), water diversions, withdrawals and salinisations; agricultural and industrial pollutions [36] of inland lake water. All these factors have led to enhanced freshwater input associated with high concentration of different salts, heavy metals, P, N and organic matter [11] which were suggested as potential drivers for the increasing appearance of microbial mat formation or algal blooms in saline lakes during summer [11,23]. Increased temperature due to global warming might play a key factor to exacerbate these challenges and vice versa [23]. Therefore, photo-induced and microbial transformation of EPS into new FDOM could be enhanced, which concurrently may impact the C and N mineralization, fluxes and cycles in inland saline lakes, freshwater lakes and oceans. Furthermore, photochemical processes are important pathways for the production of reactive oxygen species (ROS) that can be produced by interactions between sunlight and light-absorbing substances in natural waters [11]. DOM is the main source and sink of  $\cdot\text{OH}$  upon lake water irradiation, with  $[\cdot\text{OH}]$  being independent of DOM amount [24]. The DOM produced from EPS is gradually either entirely decomposed or enhanced in the aquatic environments, which is often detected in lakes, rivers [11], estuarine and marine waters [22,23]. Autochthonous DOM is generally observed at the epilimnion compared to the hypolimnion during the summer stratification period, particularly in lakes and oceans [11]. The contribution of autochthonous DOM is substantially high, approximately 0–102% in the surface waters of lakes [11]. Under the global warming scenario, if temperature continues to increase, the production of microbial EPS may also increase due to nutrient enrichment, which may eventually increase the photodegradation of the substances leading to more trace metals, ROS and recalcitrant organic matter. The production of LMW organic acids may further reduce pH and Eh condition and lead to slight acidification as observed from the present experiment.

#### 4. Conclusions

Photodegradation of EPS depends on irradiation wavelengths and intensities and exposure duration. Molecular weight (MW) of EPS is a key factor for controlling their physical, chemical, and biological characteristics in surface waters. It is evidenced from chemical and spectroscopic analyses that natural organic polymers like EPS protein molecules were comprehensively transformed from HMW to LMW organic acids in accordance with changes in the functional groups bound in EPS. The production of organic acids further lead to lowering of pH and Eh. During sunlight exposure fluorescence intensity of EPS components were found to degrade. The results from EEM-PARAFAC modelling suggested that EPS, composed of proteins and humic acids, is gradually fragmented into various components in water under photo-induced processes. Such fragmented components are gradually either

entirely decomposed or enhanced in quantity in water environments. This study therefore implies that EPS from microbial origins can increase the production of autochthonous fluorescent DOMs in natural waters and could be a key controller of the geochemistry and transportation of diverse metal pollutants in inland freshwater, saline and marine ecosystems.

#### Acknowledgements

This work was financially supported by the National Natural Science Foundation of China (41203088, 41673127, 31360027, U1120302, and 21177127). This study was also partly supported by the National Key Research and Development Program of China (2016YFA0601000) and Key Construction Program of the National "985" Project, Tianjin University, China. **Mashura Shammi and her project was supported by the CAS-TWAS President's Fellowship program 2013.**

#### Abbreviations

CDOM	Chromophoric dissolved organic matter
DOC	Dissolved organic carbon
DOM	Dissolved organic matter
EPS	Extracellular polymeric substance
Eh	Redox potential
EEM	Excitation-emission matrix
FTIR	Fourier Transform Infrared Spectroscopy
FDOM	Fluorescent dissolved organic matter
kDa	Kilodalton
LMW	Low molecular weight
MW	Molecular-weight
PARAFAC	Parallel factor
SEC	Size exclusion chromatography

#### References

- [1] H.C. Flemming, J. Wingender, U. Szewzyk, P. Steinberg, S.A. Rice, S. Kjelleberg, Biofilms: an emergent form of bacterial life, *Nat. Rev. Microbiol.* 14 (9) (2016) 563–575.
- [2] J.J. Schuster, G.H. Markx, Biofilm architecture, *Adv. Biochem. Eng. Biotechnol.* 146 (2013) 77–96.
- [3] L.J. Stal, H. Bolhuis, M.S. Cretoiu, *Phototrophic Microbial Mats*, Springer, 2017, pp. 295–318.
- [4] M. Slattery, M. Lesser, Allelopathy-mediated competition in microbial mats from antarctic lakes, *FEMS Microbiol. Ecol.* 93 (5) (2017).
- [5] T.T. More, J.S. Yadav, S. Yan, R.D. Tyagi, R.Y. Surmapalli, Extracellular polymeric substances of bacteria and their potential environmental applications, *J. Environ. Manage* 144 (2014) 1–25.
- [6] H.C. Flemming, J. Wingender, The biofilm matrix, *Nat. Rev. Microbiol.* 8 (9) (2010) 623–633.
- [7] G.P. Sheng, H.Q. Yu, X.Y. Li, Extracellular polymeric substances (EPS) of microbial aggregates in biological wastewater treatment systems: a review, *Biotechnol. Adv.* 28 (6) (2010) 882–894.
- [8] G.P. Sheng, H.Q. Yu, Characterization of extracellular polymeric substances of aerobic and anaerobic sludge using three-dimensional excitation and emission matrix fluorescence spectroscopy, *Water Res.* 40 (6) (2006) 1233–1239.
- [9] J. Wingender, T.R. Neu, H.C. Flemming, *Microbial Extracellular Polymeric Substances*, Springer, Berlin Heidelberg, 1999.
- [10] I.W. Sutherland, Biofilm exopolysaccharides: a strong and sticky framework, *Microbiology* 147 (2001) 3–9.
- [11] K.M.G. Mostofa, T. Yoshioka, M.A. Mottaleb, D. Vione (Eds.), *Photobiogeochemistry of Organic Matter: Principles and Practices in Water Environments*, Springer-Verlag, Berlin Heidelberg, 2013.
- [12] E.T. Harvey, S. Kratzer, A. Andersson, Relationships between colored dissolved organic matter and dissolved organic carbon in different coastal gradients of the Baltic Sea, *Ambio* 44 (sup 3) (2015) 392–401.
- [13] J.J. Cole, Y.T. Prairie, N.F. Caraco, W.H. McDowell, L.J. Tranvik, R.G. Striegl, C.M. Duarte, P. Kortelainen, J.A. Downing, J.J. Middelburg, J. Melack, Plumbing the global carbon cycle: integrating inland waters into the terrestrial carbon budget, *Ecosystems* 10 (1) (2007) 172–185.
- [14] T. Lou, H. Xie, Photochemical alteration of the molecular weight of dissolved organic matter, *Chemosphere* 65 (11) (2006) 2333–2342.
- [15] M.A. Moran, R.G. Zepp, Role of photoreactions in the formation of biologically labile compounds from dissolved organic matter, *Limnol. Oceanogr.* 42 (6) (1997) 1307–1316.
- [16] D. Bhatia, I. Bourven, S. Simon, F. Bordsas, E.D. van Hullebusch, S. Rossano,



- P.N. Lens, G. Guibaud, Fluorescence detection to determine proteins and humic-like substances fingerprints of exopolymeric substances (EPS) from biological sludges performed by size exclusion chromatography (SEC), *Bioresour. Technol.* 131 (2013) 159–165.
- [17] C. Kantar, H. Demiray, N.M. Dogan, C.J. Dodge, Role of microbial exopolymeric substances (EPS) on chromium sorption and transport in heterogeneous subsurface soils: I. Cr(III) complexation with EPS in aqueous solution, *Chemosphere* 82 (10) (2011) 1489–1495.
- [18] R.S. Wotton, The ubiquity and many roles of exopolymers (EPS) in aquatic systems, *Sci* 68 (suppl. 1) (Mar 2004) 13–21.
- [19] X. Zhang, P. Bishop, Biodegradability of biofilm extracellular polymeric substances, *Chemosphere* 50 (2003) 63–69.
- [20] W. Song, C. Zhao, S. Mu, X. Pan, D. Zhang, F.A. Al-Misned, M.G. Mortuza, Effects of irradiation and pH on fluorescence properties and flocculation of extracellular polymeric substances from the cyanobacterium *Chroococcus minutus*, *Colloids Surf. B* 128 (2015) 115–118.
- [21] W. Song, C. Zhao, D. Zhang, S. Mu, X. Pan, Different resistance to UV-B radiation of extracellular polymeric substances of two cyanobacteria from contrasting habitats, *Front. Microbiol.* 7 (2016) 1208.
- [22] M.A. Moran, M. Sheldon Jr., R.G. Zepp, Carbon loss and optical property changes during long-term photochemical and biological degradation of estuarine dissolved organic matter, *Limnol. Oceanogr.* 45 (2000) 1254–1264.
- [23] K.M.G. Mostofa, C.Q. Liu, D. Vione, K. Gao, H. Ogawa, Sources, factors, mechanisms and possible solutions to pollutants in marine ecosystems, *Environ. Pollut.* 182 (2013) 461–478.
- [24] D. Vione, G. Falletti, V. Maurino, C. Minero, E. Pelizzetti, M. Malandrino, R.-I. Olariu, C. Arsene, Sources and sinks of hydroxyl radicals upon irradiation of natural water samples, *Environ. Sci. Technol.* 40 (2006) 3776–3781.
- [25] M.A. Moran, R.G. Zepp, UV radiation effects on microbes and microbial processes, in: D. Kirchman (Ed.), *Microbial Ecology of the Oceans*, Wiley, New York, 2000.
- [26] P. Coble, Characterization of marine and terrestrial DOM in sea water using excitation-emission matrix spectroscopy, *Mar. Chem.* 51 (1996) 325–346.
- [27] Y. Yamashita, E. Tanoue, Chemical characterization of protein-like fluorophores in DOM in relation to aromatic amino acids, *Mar. Chem.* 82 (2003) 255–271.
- [28] M. Shammi, X.L. Pan, K.M.G. Mostofa, D. Zhang, C.Q. Liu, Photo-flocculation of microbial mat extracellular polymeric substances and their transformation into transparent exopolymer particles: chemical and spectroscopic evidences, *Sci. Rep.* 7 (1) (2017).
- [29] Y. Bai, R. Su, L. Yan, P. Yao, X. Shi, X. Wang, Characterization of chromophoric dissolved organic matter (CDOM) in the East China Sea in autumn using excitation-emission matrix (EEM) fluorescence and parallel factor analysis (PARAFAC), *Sci. China Chem.* 56 (2013) 1790–1799.
- [30] Z.G. Wang, W.Q. Liu, N.J. Zhao, H.B. Li, Y.J. Zhang, J.G. Liu, Composition analysis of colored dissolved organic matter in Taihu Lake based on three dimension excitation-emission fluorescence matrix and PARAFAC model, and the potential application in water quality monitoring, *J. Environ. Sci.* 19 (2007) 787–791.
- [31] C.A. Stedmon, S. Markager, R. Bro, Tracing dissolved organic matter in aquatic environments using a new approach to fluorescence spectroscopy, *Mar. Chem.* 82 (2003) 239–254.
- [32] R. Bro, PARAFAC Tutorial and applications, *Chemom. Intell. Lab. Syst.* 38 (1997) 149–171.
- [33] Y. Yamashita, R. Jaffé, N. Maie, E. Tanoue, Assessing the dynamics of dissolved organic matter (DOM) in coastal environments by excitation emission matrix fluorescence and parallel factor analysis (EEM-PARAFAC), *Limnol. Oceanogr.* 53 (2008) 1900–1908.
- [34] Y. Rusuli, L. Li, F. Li, M. Eziz, Water-level regulation for freshwater management of Bosten lake in Xinjiang, China, *Water Sci. Technol. Water Supply* 16 (2016) 828–836.
- [35] M. Shammi, X.L. Pan, K.M.G. Mostofa, D. Zhang, C.Q. Liu, Seasonal variations and characteristics differences in the fluorescent components of extracellular polymeric substances from mixed biofilms in saline lake, *Sci. Bull.* 62 (2017) 764–766.
- [36] G.J. Xie, J.P. Zhang, X.M. Tang, Y.P. Cai, G. Gao, Spatio-temporal heterogeneity of water quality (2010–2011) and succession patterns in Lake Bosten during the past 50 years, *J. Lake Sci.* 23 (2017) 837–846.
- [37] X. Pan, J. Liu, D. Zhang, X. Chen, L. Li, W. Song, J. Yang, A comparison of five extraction methods for extracellular polymeric substances (EPS) from biofilm by using three-dimensional excitation-emission matrix (3DEEM) fluorescence spectroscopy, *Water SA* 36 (2010) 111–116.
- [38] S. Comte, G. Guibaud, M. Baudu, Relations between extraction protocols for activated sludge extracellular polymeric substances (EPS) and EPS complexation properties, *Enzyme Microbiol. Tech.* 38 (2006) 237–245.
- [39] H. Liu, H.H.P. Fang, Extraction of extracellular polymeric substances (EPS) of sludges, *J. Biotechnol.* 95 (2002) 249–256.
- [40] M. Dubois, K. Gilles, J. Hamilton, P. Rebers, F. Smith, Colorimetric method for determination of sugars and related substances, *Anal. Chem.* 28 (1956) 350–356.
- [41] B. Frølund, R. Palmgren, K. Keiding, P.H. Nielsen, Enzymatic activity in the activated sludge floc matrix, *Water Res.* 30 (1996) 1749–1758.
- [42] N. Yee, L.G. Benning, V.R. Phoenix, F.G. Ferris, Characterization of metal-cyanobacteria sorption reactions: a combined macroscopic and infrared spectroscopic investigation, *Environ. Sci. Technol.* 38 (2004) 775–782.
- [43] S. Simon, B. Pairo, M. Villain, P. D'Abzac, E. Van Hullebusch, P. Lens, G. Guibaud, Evaluation of size exclusion chromatography (SEC) for the characterization of extracellular polymeric substances (EPS) in anaerobic granular sludges, *Bioresour. Technol.* 100 (2009) 6258–6268.
- [44] H. Liu, H.H.P. Fang, Characterization of electrostatic binding sites of extracellular polymeric substances by linear programming analysis of titration data, *Biotechnol. Bioeng.* 80 (2002) 806–811.
- [45] S. Comte, G. Guibaud, M. Baudu, Relations between extraction protocols for activated sludge extracellular polymeric substances (EPS) and complexation properties of Pb and Cd with EPS, *Enzyme Microb. Tech.* 38 (2006) 246–252.
- [46] S. Comte, G. Guibaud, M. Baudu, Biosorption properties of extracellular polymeric substances (EPS) towards Cd, Cu and Pb for different pH values, *J. Hazard Mater* 151 (2008) 185–193.
- [47] J. Hizal, R. Apak, Modeling of copper(II) and lead(II) adsorption on kaolinite-based clay minerals individually and in the presence of humic acid, *J. Colloid Interface Sci.* 295 (1) (2006) 1–13.
- [48] J. Boily, J. Fein, Proton binding to humic acids and sorption of Pb (II) and humic acid to the corundum surface, *Chem. Geol.* 168 (3) (2000) 239–253.
- [49] O. Braissant, A.W. Decho, K.M. Przekop, K.L. Gallagher, C. Glunk, C. Dupraz, P.T. Visscher, Characteristics and turnover of exopolymeric substances in a hypersaline microbial mat, *FEMS Microbiol. Ecol.* 67 (2) (2009) 293–307.
- [50] R.P. Singh, M.K. Shukla, A. Mishra, P. Kumari, C.R.K. Reddy, B. Jha, Isolation and characterization of exopolysaccharides from seaweed associated bacteria *Bacillus licheniformis*, *Carbohydr. Polym.* 84 (3) (2011) 1019–1026.
- [51] P. d'Abzac, F. Bordes, E. van Hullebusch, P.N. Lens, G. Guibaud, Effects of extraction procedures on metal binding properties of extracellular polymeric substances (EPS) from anaerobic granular sludges, *Colloids Surf. B* 80 (2) (2010) 161–168.
- [52] S. Adeleye, J.R. Conway, T. Perez, P. Rutten, A.A. Keller, Influence of extracellular polymeric substances on the long-term fate, dissolution, and speciation of copper-based nanoparticles, *Environ. Sci. Technol.* 48 (21) (2014) 12561–12568.
- [53] H. Ogawa, Y. Amagai, I. Koike, K. Kaiser, R. Benner, Production of refractory dissolved organic matter by bacteria, *Science* 292 (2001) 917–920.
- [54] T. Kawaguchi, A.W. Decho, Isolation and biochemical characterization of extracellular polymeric secretions (EPS) from modern soft marine stromatolites (Bahamas) and its inhibitory effect on CaCO<sub>3</sub> precipitation, *Prep. Biochem. Biotechnol.* 32 (1) (2002) 51–63.
- [55] A.W. Decho, P.T. Visscher, R.P. Reid, Production and cycling of natural microbial exopolymers (EPS) within a marine stromatolite, *Palaeogeogr. Palaeoclimatol. Palaeoecol.* 219 (1–2) (2005) 71–86.
- [56] D. Zhang, X. Pan, K.M.G. Mostofa, X. Chen, G. Mu, F. Wu, J. Liu, W. Song, J. Yang, Y. Liu, Q. Fu, Complexation between Hg (II) and biofilm extracellular polymeric substances: an application of fluorescence spectroscopy, *J. Hazard Mater* 175 (2010) 359–365.
- [57] D. Zhang, D.J. Lee, X. Pan, Desorption of Hg(II) and Sb(V) on extracellular polymeric substances: effects of pH, EDTA, Ca(II) and temperature shocks, *Bioresour. Technol.* 128 (2013) 711–715.